Determination of OH Number Densities Outside of a Platinum Catalyst Using Cavity Ringdown Spectroscopy†

Åsa Johansson,‡ Stina Hemdal,§ Mats Andersson,‡ and Arne Rosén*,‡

Department of Physics, Göteborg University, SE-41296 Göteborg, Sweden, and Department of Applied Physics, Chalmers University of Technology, SE-41296 Göteborg, Sweden

Received: December 31, 2006; In Final Form: March 14, 2007

It is demonstrated that cavity ringdown spectroscopy (CRDS) can be used to probe reaction intermediates desorbing from the surface during a heterogeneous catalytic reaction and provide information valuable in understanding the reaction kinetics. During water formation from H_2 and O_2, desorbed OH molecules outside of a polycrystalline platinum catalyst were quantified as a function of the relative hydrogen concentration, α_{H_2} using CRDS. The temperature of the catalyst was 1500 K, the total pressure was 26 Pa, and the flow was set to 100 sccm. At a distance of 6.5 mm from the Pt catalyst, the maximum OH concentration was found to be $1.5 \pm 0.2 \times 10^{12}$ cm^{-3} at an α_{H_2} value of 10%, and the rotational temperature was determined to be 775 ± 24 K. The desorbed OH molecules were also probed using laser-induced fluorescence (LIF), and the α_{H_2}-dependent OH abundance was compared with the CRDS results. The relative concentration of OH probed with LIF appeared to be lower at $\alpha_{H_2} = 30-50\%$ compared to what was determined by CRDS. The observed discrepancy is suggested to be due to electronic quenching, as was indicated by a shorter fluorescence lifetime at $\alpha_{H_2} = 30\%$ compared to at $\alpha_{H_2} = 10\%$.

1. Introduction

In understanding catalysis and combustion, intermediates play an important role in the overall description of reaction paths, elementary reaction rates, soot formation, and so forth.[1−4] Soot formation is a complex process where the first step is the breaking up of fuel into radicals and small molecules.[5] The radicals are often very reactive and short-lived and, therefore, exist in low concentrations, which makes them difficult to detect and quantify. The development of different laser spectroscopic techniques has given new opportunities to probe such molecules in a nonintrusive way.

The OH radical is an important intermediate in combustion, in general, and is also crucial in catalytic water formation from hydrogen and oxygen. The OH molecules are formed on the catalytic surface and rapidly react to form water. Hydrogen fuel cells use hydrogen as fuel and oxygen as the oxidant that, on the cathode, reacts to form water. The electrode plates are coated with a catalyst, for example, platinum, in order to lower the activation barrier and thereby gain a higher efficiency.

If the surface temperature is sufficiently high (>900 K) during catalytic water formation, a small fraction of OH molecules can desorb into the gas phase and be probed using laser spectroscopy. Laser-induced fluorescence (LIF) is a sensitive technique for diagnostics, imaging, and measuring relative concentrations. In LIF, the resonant laser light excites the molecules from a lower electronic state to a higher one. The molecules will then relax to the lower energy state by emitting a photon, that is, fluoresce. This method can also be used to determine rotational temperature distributions of species in combustion systems by probing several resonances.

Studies of OH radicals outside of a Pt catalyst with LIF was done for the first time in the late 1970s by the group of M.C. Lin.[6] During the 1980s, studies of OH radicals within the water formation reaction on a platinum catalyst were initiated by the Molecular Physics group at Chalmers University of Technology and Göteborg University.[7] Here follows a brief summary of their studies. The kinetics of the water formation and OH desorption rates were thoroughly investigated as a function of total pressure, hydrogen mixing ratio α_{H_2}, and catalyst temperature.[8] The relative hydrogen concentration, α_{H_2}, is defined as

$$\alpha_{H_2} = \frac{p_{H_2}}{p_{H_2} + p_{O_2}} \quad (1)$$

where p_{H_2} and p_{O_2} are the partial pressures of hydrogen and oxygen, respectively. The desorption energies of OH from Pt have also been investigated.[9,10] Information about the distribution of OH molecules outside of the catalyst could be gained by one-dimensional or two-dimensional imaging using a diode array[11] or a CCD system.[12] The OH gas-phase chemistry as a function of distance from the catalyst was investigated at sufficiently high pressures, < 2 kPa.[13,14] In order to measure the surface coverage within the H_2/O_2 reaction on Pt(111), studies using second harmonic generation (SHG)[15] were performed. To increase the understanding of the H_2/O_2 reaction at lower pressures, ≈0.01 Pa, resonance-enhanced multiphoton ionization (REMPI) was applied as a very sensitive detection method.[16]

The relative concentrations of OH outside of various noble metals known to catalyze the H_2/O_2 reaction have also been investigated.[17] It was found that the yield of OH outside of the catalyst increased with the noble metal as Ni < Ir < Rh < Pd < Pt. Moreover, laser-induced fluorescence has been utilized by several groups to study desorbed OH radicals from Pt, Pd,

† Part of the special issue "M. C. Lin Festschrift".

* To whom correspondence should be addressed. E-mail: arne.rosen@physics.gu.se.

‡ Göteborg University.

§ Chalmers University of Technology.

10.1021/jp069061v CCC: $37.00
Published on Web 04/28/2007

Ni, and Rh; see, for example, refs 8,13,18−22. Even though much important information about the H_2/O_2 system has been accomplished with LIF, there are only a few tentative attempts to extract quantitative number densities of OH outside of Pt mainly due to difficulties in determining the fluorescence quantum yield.[14,23]

In addition to the experiments, theoretical models were early developed in order to understand the kinetics of water formation in more detail. Simultaneous probing of OH desorption and water formation reduced the number of parameters to be fitted into a theoretical model. The initial models were based on a simple Langmuir−Hinshelwood-type kinetic model. Water was believed to form from a sequential addition of atomic hydrogen, where the following reaction steps were included: $H_2 \rightleftharpoons 2H^*$, $O_2 \rightarrow 2O^*$, $O^* + H^* \rightarrow OH^*$, $H^* + OH^* \rightarrow H_2O^* \rightarrow H_2O$, and $OH^* \rightarrow OH$; the asterisk denotes adsorbed on the surface. This model could relatively well predict the α_{H_2} values for which maxima in OH desorption and water formation were measured,[24] but the overall agreement with the α_{H_2} dependence of the desorption rates was insufficient. An improved model, in which the OH and water formation reactions were made reversible, could much better reproduce the OH desorption rate as a function of α_{H_2} for all α_{H_2} values.[25,26] The coverage of intermediates could be predicted, and therefore, the apparent desorption energy as a function of α_{H_2} could also be modeled and fitted to experimental data.[27] Kinetic Monte Carlo simulations, with a finite diffusion of adsorbed hydrogen atoms, has also been applied to analyze the OH desorption rate.[28] Below the desorption temperature of water ($T_{des} \approx 170$ K), a mechanism with an autocatalytic behavior has been suggested.[29] The adsorbed OH was monitored with STM and seen to migrate over the Pt(111) surface in a kinetic wave. Even though much has been accomplished, there are uncertainties; the reaction paths and values for desorption and formation energies on Pt are debated.[30,31]

Knowledge about quantitative concentrations is important for successful comparisons with simulations. Absolute number densities give valuable information when determining rate constants and are preferred for a detailed understanding of the complex chemistry on the catalytic surface. To complement the extensive LIF studies and to encourage further modeling of the H_2/O_2 system, the abundance of OH outside of a polycrystalline platinum catalyst has, in this work, been quantified as a function of α_{H_2} using cavity ringdown spectroscopy (CRDS).

This method, CRDS, is a highly sensitive absorption method well suited for measuring reaction intermediates in trace amounts.[3,32] The only prerequisites for CRDS to work are that the species of interest absorb light at an accessible wavelength and that there is no interference from other species at this wavelength. This technique, in contrast to LIF, can also be applied even if the excited state of the probed molecule does not fluoresce. Because of its long absorption path length, CRDS is also much more sensitive than conventional absorption methods such as FTIR.[33]

There are a few studies of combined LIF and CRDS,[32,34−43] mostly of flames. An advantage of combining the LIF and CRDS techniques for flames is that the absorption path length, necessary to calculate the number density in CRDS, can be obtained directly if the fluorescence light is imaged with a CCD camera.

In a previous study,[44] we showed for the first time that CRDS also could be utilized to quantify OH molecules desorbing from the surface during catalytic water formation. The rotational temperature and the amount of OH 6.5 *mm* outside the Pt catalyst at $\alpha_{H2} \approx 10\%$ was calculated.

The objective of this study was to use CRDS to quantify the amount of OH outside of a polycrystalline platinum catalyst as a function of α_{H_2}. The number densities obtained in the CRDS measurements were also compared with a LIF experiment. With the availability of exact concentrations of the OH radical in catalytic water formation, we encourage further developments of theoretical models to increase the understanding of the system.

The CRDS method and some examples of combined CRDS and LIF measurements will be discussed in section 2, followed by a detailed explanation of the experimental setup in section 3. The Results and Discussion, section 4, contains the CRDS measurements in comparison to quantifications of OH outside of a Pt catalyst using LIF. The influence of electronic quenching will also be assessed.

2. Cavity Ringdown Spectroscopy

Cavity ringdown spectroscopy is an optical absorption technique which was developed from mirror reflectivity measurements and was first demonstrated by O'Keefe and Deacon in 1988 measuring transitions in molecular oxygen.[45] CRDS was introduced in combustion science about 13 years ago by Meijer et al.[46] The temperature in a Bunsen burner flame was determined to 1900 K by probing OH with CRDS. At about the same time, Yu and Lin[47,48] used CRDS to study time-resolved kinetics of phenyl radical reactions. An overview of those measurements can also be found in ref 32. All 190 CRDS studies published until June 2000 were summarized in ref 49. Cavity ringdown spectroscopy has been applied in a wide spectral range from 205 to 10690 nm and in numerous applications, from studies of quantum chemistry[43] to more commercial applications.[50]

Until the year 2000, OH molecules were only quantified in flames. The CRDS technique is also independent of electronic quenching, in contrast to, for example, fluorescence methods such as LIF;[3] for reviews, see refs 49,51−53.

2.1. Principles of the Method. Basically, a light pulse is injected into an optical cavity consisting of two mirrors of high reflectivity. Due to the low transmittance of the mirrors, the intensity of the light will decay as it travels back and forth inside the cavity. The intensity of the transmitted light at the output mirror is detected as a function of time. The time it takes for the light to decay to 1/e of the original intensity is called the ringdown time. Ideally, the decay time depends on the reflectivity, *R*, and the spacing, *L*, of the mirrors. If the wavelength of the light coincides with a transition of a molecule present inside the cavity, the decay of the light will occur faster due to absorption. In this way, the absorbance, *A*, given by the Lambert−Beer law

$$A = \sigma \cdot l_s \cdot N_J \tag{2}$$

can be measured by comparing the ringdown time for on and off resonance, according to eq 3

$$A = \frac{L}{c}\left(\frac{1}{\tau_{on}} - \frac{1}{\tau_{off}}\right) \tag{3}$$

where σ is the absorption cross section, l_s the absorption path length, N_J the number density of molecules at the rotational level J, c the speed of light, and τ_{on} and τ_{off} are the ringdown times for the laser light tuned on and off resonance, respectively. By assuming a Boltzmann distribution, the total number density of

a diatomic molecule in the vibrational ground state, N_{tot}, can be calculated if the temperature of the gas is known, according to eq 4

$$N_{tot} = \frac{N_J \dfrac{k_B T}{hcB_e}}{(2J+1)e^{-(B_e J(J+1)hc)/k_B T}} \quad (4)$$

where k_B is the Boltzmann constant, T the temperature, h is Planck's constant, B_e the rotational constant, and J is the rotational quantum number.

The sensitivity of CRDS is dependent on the reflectivity of the mirrors and the accuracy in determining the ringdown time, τ. The minimum absorbance to be measured by CRDS is given by eq 5[54]

$$[\sigma \cdot l_s \cdot N_J]_{min} = (1-R)\frac{\Delta\tau}{\tau} \quad (5)$$

where R is the mirror reflectivity, $\Delta\tau$ is the minimum change in ringdown time that can be measured, and τ is the ringdown time.

The CRDS technique is based on the assumption of a single-exponential decay of the intensity. Multiexponential decay occurs if the light in the cavity, for some reason, takes different paths and therefore decays unequally. This may occur due to mode formation or bandwidth relations between the laser and the absorbing molecule. Under such circumstances, the ringdown time evaluation will be inaccurate if calculated with a single-exponential fit. CRDS becomes less accurate as the absorption intensity increases since the decay time is shorter for larger absorption. This makes the method unsuitable for measuring high absorption since an optical depth problem will occur.

2.2. Applications of Combined CRDS and LIF. Laser-induced fluorescence is a good tool for gaining information about spatial resolution and relative concentrations of a species.The laser beam can be expanded into a sheet, allowing the two-dimensional imaging of the species. This is often referred to as planar LIF. However, for quantitative measurements, LIF needs some kind of calibration.

By combining CRDS and LIF, the relative strengths of both methods can be utilized. For example, the absorption path length, needed for calculations of CRDS number densities, can be estimated from an ICCD image of the fluorescence. On the other hand, cavity ringdown spectroscopy can provide absolute number densities, without calibration, along the line of sight.

There is an increasing number of joint CRDS and LIF studies presented, and some examples are summarized here.

One of the first combined CRDS and LIF studies was performed by Spaanjaars et al.[34] They performed simultaneous LIF and CRDS measurements to obtain precise values for the relative predissociation lifetimes of OH in a laminar CH_4/air flame. The predissociation rate was obtained from the ratio of the absorption and the fluorescence signal. The molecules were excited by a 284 nm beam from a dye laser. The beam was split into a low-intensity beam directed into the cavity of the CRDS setup and a high-intensity beam for the LIF measurement. The obtained results for the relative quantum yields and lifetimes were compared to calculated values and showed an overall agreement.

Mercier et al.[35] used CRDS and LIF to study OH radicals in two atmospheric burners a premixed flat flame burner and a Wolfhard−Parker burner. The OH concentration was measured as a function of the transverse position in the flames for different heights. The achieved quantitative profiles were compared to LIF profiles by normalizing the LIF profile to the peak value of the obtained CRDS profile. The CRDS and LIF measurements were conducted separately at around 306 nm. The premixed flame was analyzed by probing the $R_1(7)$ transition in the A−X(1-0) band and by collecting the fluorescence of the (0-0) and (1-1) bands. In the Wolfhard−Parker burner, both CRDS and LIF data was collected by exciting the $R_{21}(12)$ transition of the (0-0) band. The maximum OH number density was calculated to be 2.5×10^{14} cm^{-3} at 6 mm above the Wolfhard−Parker burner. The same group has performed plenty of CRDS studies in flames probing different radicals and some combined CRDS−LIF experiments probing, for example, NO.[36]

Dreyer et al.[37] probed OH molecules with LIF and CRDS in a laminar methane−air flame at atmospheric pressures. Experimental data were also compared with theoretical calculations using the PREMIX code. The LIF and CRDS experiments were not performed simultaneously. Light from a frequency-doubled pulsed dye laser at wavelengths near 302.5 nm was used to study the OH molecules. The temperature of the flame was determined with CRDS to be 2021 ± 55 K at an equivalence ratio of 0.99. At 1 cm above the burner, the concentration of OH was determined with CRDS to be ≈3000 ppm. This result was also confirmed using LIF and kinetic modeling.

Cavity ringdown spectroscopy was also applied for the quantitative detection of CH in atmospheric flames.[38] The rotational temperature was derived from the measured Boltzmann distribution, and the obtained CH density profiles were compared with calculated densities. The CRDS data were compared to older LIF profiles measured on the same flame.

A combination of LIF and CRDS was also used to study CN and CH molecules in a low-pressure (3.3 kPa) methane−air−nitrogen flame.[39] Both molecules were detected using a pulsed dye laser at 388 nm. Planar LIF was used to obtain spatially resolved fluorescence detection. The maximum CH concentration was determined to be $\approx 1.25 \times 10^{12}$ cm^{-3}, 45 mm above the burner head. The maximum number density of CN was found to be $\approx 1.2 \times 10^{9}$ cm^{-3}, 60 mm above the burner. These results were also compared to measurements using a NO-seeded flame. Calculations of the number densities using the PREMIX code and the GRI−Mech 3.0 model were also presented.

In a more recent publication by Luque et al.,[40] CH radicals in a low-pressure methane−air flame were simultaneously monitored with LIF and CRDS. The CH molecules were excited with laser light near 430 nm. Simultaneous with the CRDS experiments, the spatial distribution of CH molecules was probed with LIF using a CCD camera. The 2D-LIF images were also a helpful tool to control the alignment of the cavity. The number density of CH as a function of distance from the burner was measured. The maximum CH number density was found to be about 1.3×10^{12} cm^{-3}, 0.5 cm above the burner.

CH concentrations in flames using both LIF and CRDS were also studied by Naik and Laurendeau.[41] They used three premixed methane−air flames with different mixing ratios and a single non-premixed methane−air flame, all at atmospheric pressure. For both the CRDS and LIF studies, the $Q_1(10)$ transition at 431.5 nm in the A−X(0,0) band was probed. The LIF measurements were used to determine the optical path length. Number densities of CH were determined from the CRDS measurements and presented together with simulations. Depending on the mixing ratio, the maximum CH concentration was found at different distances from the fuel nozzle. The maximum CH concentration was found to be about 1 ppm at 2 mm from the nozzle. The number densities obtained from the

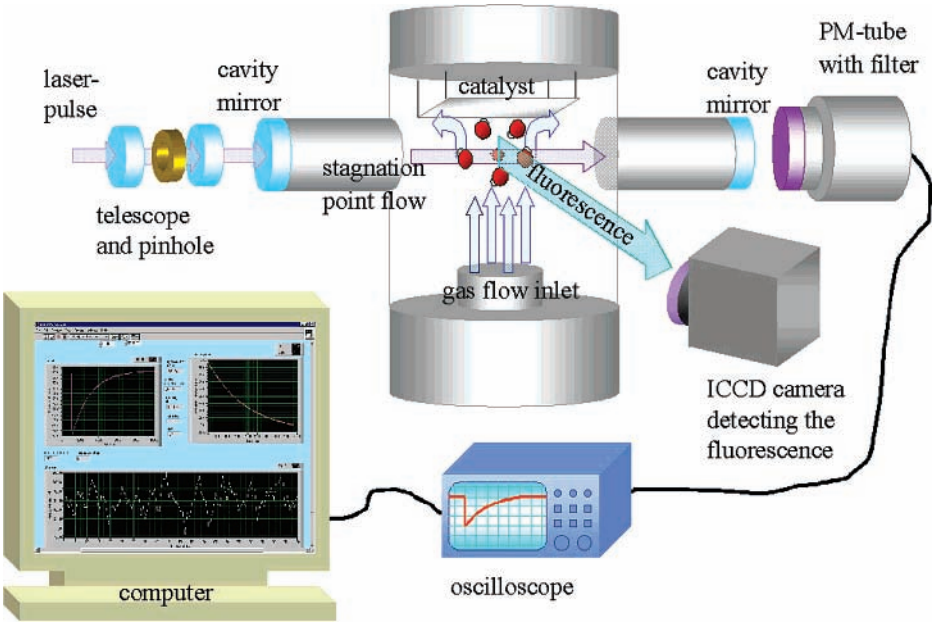

Figure 1. The experimental setup used for the CRDS and LIF measurements of OH molecules outside of the Pt catalyst. The laser pulse enters from the left. During the LIF experiment, the mirrors were replaced with quartz glass windows. The ICCD camera was also connected to a computer.

simulations showed a good agreement with the CRDS and LIF results.

In a recent study by Bahrini et al., CaBr and CaI radicals were studied with CRDS and LIF.[42] With these techniques, the radicals could be studied at much lower temperatures (about 350 K) than those previously reported (1300−2000 K). The CaBr radical was studied in the 620−640 nm wavelength range, and the CaI radical was studied around 420−440 nm. They found that a comparison of the LIF and CRDS spectra, recorded simultaneously or at the same experimental conditions, could be a sensitive test to detect predissociation within the molecules. A good correlation between the CRDS and LIF spectra was noted, but no number densities were calculated.

3. Experimental Section

The H_2/O_2 reaction was probed inside a Roots-pumped (Balzers WKP 250 A) stainless steel chamber. The flow of hydrogen and oxygen gases was regulated with two mass flow controllers (Vacuum General FC6-21), one for each gas. The total gas flow was set to 100 sccm (1 sccm = 1 standard cubic centimeter per minute $\approx 4 \times 10^{17}$ molecules/s at 300 K, which was the temperature of the gas at the inlet). The gases were mixed and entered the chamber through an orifice, 20 mm in diameter, 30 mm below the catalyst. This geometry gave a stagnation point flow field below the catalyst; see, for example, Figure 1 in ref 30. The gas composition at the inlet was calibrated with a quadrupole mass spectrometer (Balzers QMG 420) located in an adjacent turbo-pumped chamber. The total gas pressure in the main chamber was measured with a capacitance manometer (MKS 227AAG) and kept constant at 26 Pa. A schematic overview of the experimental setup is shown in Figure 1.

The catalyst was mounted in a tantalum holder and heated resistively. Polycrystalline platinum foils (Goodfellow 99.95% Pt) with the dimensions $3.8 \times 21 \times 0.025$ mm were used. The temperature was determined by measuring the resistance of the foil and was kept constant with a Labview-based controller.

For both the CRDS and LIF experiments, frequency-doubled light from an excimer-pumped dye laser (Lambda Physik EMG 102 E and Lambda Physik FL 2002 E) was used to study the OH molecules. The bandwidth of the laser light was 0.2 cm^{-1}, and the duration of the laser pulses was 10 ns, according to specifications. The laser light had a wavelength of about 307 nm. The $R_1(4)$ transition in the $X^2\Pi(v'' = 0) \leftarrow A^2\Sigma^+(v' = 0)$ band of the OH molecule was used both in the CRDS and LIF experiments. When the rotational temperature was determined, several transitions in the R_1 branch were studied.[44]

For the CRDS study, highly reflecting mirrors with a 6 m radius of curvature (Los Gatos Research) were used. The mirrors were placed in mirror mounts at the end flanges of the reaction chamber; the mirrors also served as windows to the vacuum chamber. The separation of the mirrors was 1 m, and they had a diameter of 20 mm. The reflectivity, R, of the mirrors was 99.93% at 307 nm. The laser beam was spatially filtered using two quartz lenses and a 50 μm high-energy pinhole (Newport) before entering the cavity. The absorption path length, l_s, was estimated to be 21 mm. The mode-filtered laser beam had a diameter of about 2 mm and passed 6.5 mm below the platinum foil. The pulse energy of the laser light was around 0.06 mJ before entering the pinhole but substantially less after passing it. The transmitted light was detected with a photomultiplier tube (Thorn EMI 9558QB) mounted in a cooling house and connected to an oscilloscope (Tektronix TDS 220). A UG11 filter was placed in front of the photomultiplier tube to reduce background light. The CRDS signal was averaged four times in the oscilloscope and read out by a computer using a GPIB interface. The ringdown time was determined by fitting a single-exponential curve to the portion of the CRDS signal between 90 and 10% of the maximum intensity. This approach also reduced the influence of the non-Gaussian parts of the laser beam. For each data point, a hundred decay curves were sampled and evaluated individually. Even though the bandwidth of the laser light and the bandwidth of the Voigt profile of the $R_1(4)$ transition in the OH molecule were of the same order of magnitude, a single-exponential decay could be fitted with a good agreement. In general, for Lambert−Beer law to apply, the bandwidth of the laser must be narrower than the bandwidth of the absorbing molecule. For CRDS, however, a weaker condition also holds; if the loss due to absorption is less than the total loss of the cavity, an effective absorption coefficient

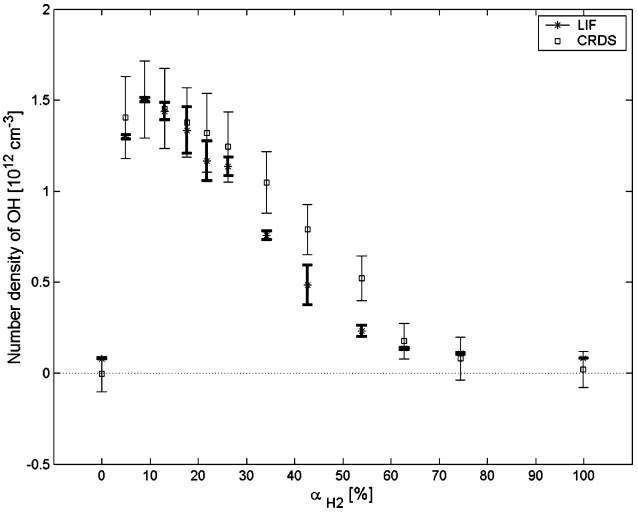

Figure 2. The OH number density measured with CRDS (square) and LIF (asterisk) as a function of α_{H_2}. The LIF data are normalized so that the maximum in OH intensity at $\alpha_{H_2} = 10\%$ coincides with the CRDS experiments. The error bars for the LIF experiment are shown in bold.

can still be determined by fitting an exponential to the decay curve.[54] The numerical constants for the OH molecule used to calculate N_{tot} originate from the simulation/database program LIFBASE.[55]

The CDRS and LIF experiments were not performed simultaneously, and in order to have geometries and conditions as identical as possible, the mode matching optics were kept during the LIF experiments. The mirrors were replaced with quartz glass windows, and the exit window was mounted in the Brewster angle to avoid reflections. The fluorescence was measured perpendicularly to the laser beam with an ICCD camera (Princeton Instruments). Data from the ICCD camera was stored on a computer and analyzed using Matlab.

4. Results and Discussion

The amount of OH outside of the catalyst depends primarily on the temperature of the catalyst, the pressure in the reactant chamber, the distance from the catalyst, and the gas composition α_{H_2}.[8,14] The flux of OH, I_{OH}, from the catalyst is described by an Arrhenius expression

$$I_{OH} = \theta_{OH}(T) A_{OH} e^{-(E^d_{OH}/k_B T)} \quad (6)$$

where $\theta_{OH}(T)$ is the temperature-dependent coverage, A_{OH} is the pre-exponential, E^d_{OH} is the desorption energy, k_B is Boltzmann constant, and T is the temperature. Due to the exponential behavior, a small change in temperature can give a drastic change in the flux of OH. For this reason, a high catalyst temperature of 1500 K was used to obtain a good OH detection efficiency with CRDS throughout the whole α_{H_2} range.

The concentration of OH versus α_{H_2} is presented in Figure 2. The temperature of the catalyst was 1500 K, the total pressure was 26 Pa, and the gas flow was set to 100 sccm. A single exponential was successfully used to fit the decay of the transmitted light in the CRDS experiment. The rather large uncertainties in the concentrations represented by the error bars in Figure 2 are caused by shot-to-shot fluctuations, which are believed to be due to vibrations of the mirrors induced by the vacuum pumps. The ringdown time off resonance was $\tau_{off} = 2600$ ns, with an uncertainty $\Delta\tau$ of 65 ns. Using those values, the minimum detectable losses per pass could be calculated from eq 5 to be $\approx 2 \times 10^{-5}$. An optimal value would be on the order of 10^{-7}.[54]

The temperature of the gas can be obtained from the slope of a Boltzmann plot ($\ln(N_J)/(2J+1)$ versus $B_e J(J+1)$). The data points falling onto a straight line would indicate thermal equilibrium. The rotational temperature of the OH molecules 6.5 mm outside of the catalyst has previously been determined to be 775 ± 24 K[44] at $\alpha_{H_2} \approx 10\%$ using CRDS, at the same experimental conditions used in this study. A rotational temperature of 775 K was also confirmed with LIF in this work

By measuring the ringdown time for the $R_1(4)$ transition and using the temperature value of 775 K, the total number density of OH as a function of α_{H_2} could be calculated 6.5 mm outside of the Pt catalyst. The amount of OH increased with increasing H_2 concentration to a maximum at an α_{H_2} value around 10%; thereafter, the measured yield of OH decreased with increasing α_{H_2}. At the reaction conditions applied in this work, the maximum OH concentration was found to be $1.5 \pm 0.2 \times 10^{12}$ cm^{-3} at $\alpha_{H_2} = 10\%$. At $\alpha_{H_2} = 40\%$, the OH number density had decreased to approximately half of the maximum value.

The rotational temperature may not be exactly the same for all α_{H_2}, but the population at the probed rotational state is only weakly dependent on the temperature.[14] For example, an increase in rotational temperature by 100 K would only give an increase of about 4% in the determined OH concentration, according to eq 4. Therefore, possible variations in the rotational temperature are not believed to influence the general shape of the OH yield versus α_{H_2} dependence in Figure 2.

The OH desorption rate during the H_2/O_2 reaction as a function of α_{H_2} has previously been measured by Fridell et al.[9] The α_{H_2}-dependent OH desorption rate from Pt(111) was measured at four different temperatures between 1100 and 1400 K and at a pressure of 6.5 Pa. The maximum OH desorption rate was found for $\alpha_{H_2} \approx 8\%$ and showed a small shift to higher α_{H_2} values with increasing temperature. The biggest change with temperature in the OH desorption rate versus α_{H_2} curves on Pt(111) was that the peak broadened significantly on the hydrogen-rich side. The half-maximum shifted from $\alpha_{H_2} \approx 15\%$ at 1100 K to an α_{H_2} larger than 30% at 1400 K. The higher increase in OH desorption rate at high α_{H_2} was explained by a higher apparent activation energy for OH desorption resulting in a stronger temperature dependence at the higher α_{H_2} values. The data recorded in this study at a surface temperature of 1500 K on a polycrystalline foil, with a maximum at $\alpha_{H_2} \approx 10\%$ and a half-maximum at $\alpha_{H_2} \approx 40\%$, is fully consistent with extrapolating the temperature trends from the study on Pt(111), and the general features of the curve presented in Figure 2 agree well with the trend found by Fridell et al.

For comparison, the relative OH concentration as a function of α_{H_2} was also probed with LIF, applying the same experimental conditions. The LIF data plotted in Figure 2 was first normalized to unity at $\alpha_{H_2} = 10\%$ and then by the maximum OH concentration from the CRDS experiment. In the hydrogen-rich part of the OH desorption versus α_{H_2} curve, there is a discrepancy between the LIF and CRDS data, which is most pronounced at α_{H_2} values between 30−50%. This deviation between the measured CRDS and LIF curves is reproducible and is probably due to influence of electronic quenching, which will be discussed below.

4.1. Electronic Quenching. The fluorescence light detected in the LIF experiment comes from spontaneous emission from the first excited electronic state to various rotational states within the ground electronic state of the OH molecule. However,

radiationless de-excitations can also occur via collisions with other molecules, which is called electronic quenching. The electronic quenching depends primarily on the pressure and the composition of the gas mixture in the chamber. The quenching rate, Q, is defined as[56]

$$Q = \sum_{i} k_q(i) n_i \quad (7)$$

where $k_q(i)$ is the quenching rate constant of species i and n_i is the number density of i. The quenching rate can be calculated if the lifetime, τ_{LIF}, of the excited state is known; see eq 8

$$\tau_{LIF} = \frac{1}{A + Q} \quad (8)$$

The Einstein A coefficient is 1/0.71 μs for the $R_1(4)$ transition used in this study; see Figure 2 in ref 57. The lifetime, τ_{LIF}, is defined as the time it takes for the intensity to decrease to 1/e of its original intensity and can be obtained from the LIF data.[58] The integrated intensity of fluorescence light is proportional to the lifetime. In the ideal case, the quenching rate, Q, is small, the lifetime of the excited state, τ_{LIF}, approaches the natural lifetime 1/A, and the observed fluorescence intensity can be assumed to be proportional to the number of excited molecules. Otherwise, the total fluorescence yield is proportional to τ_{LIF}.

In this study, the lifetime, τ_{LIF}, of OH was measured at $\alpha_{H_2} = 10$ and 30% using LIF and was found to be 0.52 ± 0.02 and 0.45 ± 0.02 μs, respectively. Lifetimes for OH have previously been determined as a function of pressure (0−13 Pa) at $\alpha_{H_2} =$ 10% by Fridell et al.[58] An extrapolation from those data shows that our measured lifetimes are in reasonable agreement.

OH has a larger quenching rate constant with water in comparison to that with oxygen and hydrogen; see, for example, Table 2 in ref 59 or in ref 58. An overview of the literature of electronic quenching of OH molecules can be found in ref 60. In a separate study, the quenching of OH in a stoichiometric $H_2/O_2/N_2O$ flame was believed to be a result of collisions with water molecules.[61] In our experiment, the maximum water production rate has its maximum on the hydrogen-rich side of the OH desorption rate maximum. This is in agreement with previous studies at various reaction conditions showing a maximum in the water production rate at an α_{H_2} value somewhere between 15 and 40%.[8,16,24] The shorter lifetime at $\alpha_{H_2} = 30\%$ compared to that at $\alpha_{H_2} = 10\%$ can, thus, be explained by a higher rate of electronic quenching due to an increased water presence. The stronger quenching is also the likely reason for the LIF signal in Figure 2 showing a relatively lower intensity than the OH abundance determined from the CRDS signal at the hydrogen-rich side of the OH desorption rate maximum.

4.2. Comparison of the OH Number Densities. There are a few previous attempts to quantitatively determine the OH concentration outside of a Pt catalyst using LIF.[14,23] However, they were performed at a single value of α_{H_2} and at different pressures and temperatures of the catalyst than those used in this study. Gudmundson et al.[14] estimated the maximum OH concentration to be $4 \times 10^{10\pm1}$ cm^{-3} at $\alpha_{H_2} = 10\%$, 130 Pa, and 1 mm outside of a 1300 K polycrystalline Pt foil in a combined LIF and modeling study. In another study,[23] the OH number density at $\alpha_{H_2} = 5\%$ was approximated from LIF data to be $2 \times 10^{7\pm1}$ cm^{-3}, 2 mm outside of the Pt foil. The temperature of the catalyst was 1100 K, and the total pressure was 1.3 Pa. Our results compared to the previous results are summarized in Table 1. The number densities presented in this study are all higher than those reported in the previous ones, but the temperature of our catalyst was much higher. A higher catalyst temperature will give a higher flux of OH, according to eq 6. Assuming a desorption energy of OH of 193 kJ/mol,[10] the factor $e^{-(E_{OH}^{d}/k_B T)}$ increases approximately 25 times if the temperature is increased from 1100 to 1300 K and increases further by a factor of 11 when going from 1300 to 1500 K. The OH coverage also has a temperature dependence, but this has a relatively limited influence. At $\alpha_{H_2} = 10\%$, the coverage of OH is ≈1.5 times higher at a surface temperature of 1100 K compared to that at 1400 K,[9] which is a small change compared to the strong dependence on the exponential term including the activation energy for desorption described above. The sticking probabilities of the reactants are also not expected to change substantially in the 1100−1500 K range.

TABLE 1: A Summary of Quantitative OH Measurements Outside of a Pt Catalyst

ref	T (K)	P (Pa)	α_{H_2} (%)	distance (mm)	N_{OH} (cm^{-3})
23	1100	1.3	5	2	$2 \times 10^{7\pm1}$
14	1300	130	10	1	$4 \times 10^{10\pm1}$
this work	1500	26	8	6.5	$1.5 \pm 0.2 \times 10^{12}$

A higher pressure is expected to lead to a higher rate of OH and water formation and desorption due to a higher flux of reactants to the catalyst surface. However, the OH and water formation rates may not be proportional to the pressure for several reasons. Mass transport effects can occur at high pressures and/or low flows, limiting the amount of reactants outside of the surface. Furthermore, if the surface coverage is sufficiently high (more than about 10%), surface sites for adsorption of reactants are blocked, and the sticking probability decreases with increasing coverage. For α_{H_2} being 10% or less, the surface coverage is dominated by oxygen atoms, but at high temperatures and/or low pressures, the total coverage is low. Another effect of changing the coverage by varying the reactant pressure is that the relative rates of reaction and desorption change. This means that an increasing pressure and, thereby, surface coverage can lead to a more rapid formation and consumption of intermediates in surface reactions. Thus, the total water production rate may increase without the OH coverage, and desorption rate, increasing in proportion.

In a study by Gudmundson et al.,[12] the dependence of the OH desorption rate as a function of pressure, up to 26 Pa, was analyzed at a catalyst temperature of 1300 K, and an almost linear dependence on the pressure was found in this pressure range. At a catalyst temperature of 1200 K, Ljungström et al.[8] also found an almost linear OH desorption rate up to a pressure of 13 Pa but then reported a slower increase, reaching a maximum at 78 Pa, and then a decrease in the OH desorption rate for higher pressures. A similar pressure dependence was also reported for a catalyst temperature of 1050 K.[7]

Finally, the distance from the surface to the point of the OH detection is different in the three studies. The OH concentration will generally decrease with increasing distance, and the OH density at a certain distance is dependent on the OH diffusion rate and the flow of reactant gases.[12] However, at short distances, the OH number density may actually increase with distance due to the temperature gradient. Gudmundson et al. investigated the influence of the flow on the OH density profile outside of a Pt catalyst at 1300 K, a pressure of 13 Pa, and $\alpha_{H_2} = 10\%$.[12] They found that at these conditions, the OH density profile was the same for direct and indirect flow, at a flow of 65 sccm, while at a flow of 760 sccm, there was a much steeper concentration gradient for the direct flow. Up to flows of about 300 sccm,

the concentration gradient was independent of the flow. Therefore, we assume that the flow does not play a role for the OH density gradient in our study or in the study of Wahnström et al.,[23] and the density profile was directly imaged in the study by Gudmundson et al.[14] At short distances from the surface such as 1 or 2 mm, the concentration is close to the maximum value, whereas it is expected to have decreased at the longer distance of 6.5 mm used in our study. If only diffusion is involved, the concentration gradient can be relatively flat, with a decrease by only about 50% at a distance of 5 mm and a pressure of 13 Pa.[12] It is therefore reasonable to assume that the OH density at the 26 Pa used in our study is between 20 and 50% of what it is at 1 or 2 mm from the catalyst surface.

After analyzing the influence of the different factors, temperature, pressure, and distance, we can make the final comparison of the numbers presented in the three studies. Our reported value for the OH number density is a factor of 38 higher than the value reported by Gudmundson et al. and a factor of 7.5×10^4 higher than that reported by Wahnström et al. In both cases, the combined error bars are just over 1 order of magnitude. Compared to the study of Gudmundson et al., we would expect a factor of 11 higher OH density due to the higher temperature. The influence of pressure is difficult to estimate since, at a pressure of 130 Pa, the increase in the OH desorption rate is likely no longer linear with pressure, and it might even be in a range where the OH yield decreases with increasing pressure. Thus, a factor of 5 higher difference in desorption rate is therefore not expected to be caused by the different pressures, even if the pressure difference is likely to still favor a higher OH desorption rate at 130 Pa compared to that at 26 Pa. The difference in distance from the foil is, as described above, expected to result in a OH number density difference of a factor of 0.2−0.5. Thus, a simple analysis of the kinetic parameters predicts an estimated OH density difference between 1 and 5 rather than the reported ratio of 38. The difference lies just inside or just outside of the estimated error margins.

A comparison with the study of Wahnström et al. yields a similar result, that is, the difference expected from the simple analysis of the kinetic parameters (approximately a factor of 275 from temperature, a factor of 20 from pressure, and a factor of 0.5 from distance) results in a ratio that is again just over 1 order of magnitude different from the ratio of the reported values.

One possible reason for the discrepancies is that an extrapolation of the influence of individual kinetic parameters is too simplified. For example, the lower surface coverage in the present study, due to a higher temperature and/or lower pressure, might more strongly favor OH desorption compared to water formation and desorption than this simple analysis indicates. In addition, uncertainties in used values such as the desorption energy of OH will also influence the results. Another reason can be that an estimate of absolute number densities from LIF measurements is difficult, as indicated by the order of magnitude error estimate, and some factor in the calibration procedure might have been under- or overestimated. The difficulty in determining accurate absolute numbers from LIF measurements does, however, emphasize the importance of access to sensitive absorption-based methods for quantification.

5. Conclusions

In this study, we have quantified desorbed OH radicals outside of a Pt catalyst as a function of α_{H_2} using cavity ringdown spectroscopy. The CRDS result was also compared with a LIF experiment at the same experimental conditions. The maximum OH concentration was found to be $1.5 \pm 0.2 \times 10^{12}$ cm^{-3} at $\alpha_{H_2} = 10\%$; at $\alpha_{H_2} = 40\%$, the OH number density had approximately decreased to half of the maximum value. The LIF and CRDS curves had the same general shape, with the maximum in OH desorption at about $\alpha_{H_2} = 10\%$, but there was a discrepancy between the LIF and CRDS curves. At the hydrogen-rich side of the OH desorption maximum, the LIF data showed a lower OH concentration compared to that from the CRDS data. This difference is reproducible and is largest for α_{H_2} values between 30 and 50%. It is suggested to be a result of an α_{H_2}-dependent quenching efficiency of the excited OH molecules. The lifetime of the excited OH molecule was measured at $\alpha_{H_2} = 10$ and 30%, and a shorter lifetime, indicating a higher quenching rate, was found at $\alpha_{H_2} = 30\%$. The absolute OH densities measured by CRDS in this study are higher than corresponding densities reported in previous LIF studies, which appears to be the case also when the influence of different reaction parameters is considered. The difference may either be due to the fact that the OH desorption rate changes nonlinearly with the reaction parameters or due to the inherent difficulty in correctly determining number densities from fluorescence measurements. In either case, the availability of absolute concentration determinations by CRDS can provide valuable input to analyze the reaction kinetics.

Acknowledgment. We gratefully acknowledge financial support from the Swedish Research Council (VR) (Contract 629-2001-4925) and CERC (Combustion Engine Research Centre). We are also thankful to PREEM for support to experimental equipment. In addition, we would like to thank Dr. Michael Försth for his contributions to the initial phase of this project.

References and Notes

(1) Warnatz, J.; Maas, U.; Dibble, R. W. *Combustion: Physical and Chemical Fundamentals, Modeling and Simulation, Experiments, Pollutant Formation*; Springer-Verlag: Berlin, Germany, 1996.
(2) Pilling, M. J.; Seakins, P. W. *Reacion Kinetics*; Oxford University Press: Oxford, U.K., 1996.
(3) Kohse-Höinghaus, K.; Jeffries, J. B. *Applied Combustion Diagnostics*; Taylor & Francis: New York, 2002.
(4) Glassman, I. *Combustion*; Academic Press: San Diego, CA, 1996.
(5) Bockhorn, H. *Soot Formation in Combustion*; Springer-Verlag: Berlin, Heidelberg, Germany, 1994.
(6) Talley, L. D.; Tevault, D. E.; Lin, M. C. *Chem. Phys. Lett.* **1979**, *66*, 584.
(7) Rosén, A.; Ljungström, S.; Wahnström, T.; Kasemo, B. *J. Electron Spectrosc. Relat. Phenom.* **1986**, *39*, 15.
(8) Ljungström, S.; Kasemo, B.; Rosén, A.; Wahnström, T.; Fridell, E. *Surf. Sci.* **1989**, *216*, 63.
(9) Fridell, E.; Elg, A.-P.; Rosén, A.; Kasemo, B. *J. Chem. Phys.* **1995**, *102*, 5827.
(10) Wahnström, T.; Fridell, E.; Ljungström, S.; Hellsing, B.; Kasemo, B.; Rosén, A. *Surf. Sci. Lett.* **1989**, *223*, L905.
(11) Fridell, E.; Westblom, U.; Aldén, M.; Rosén, A. *J. Catal.* **1991**, *128*, 92.
(12) Gudmundson, F.; Fridell, E.; Rosén, A.; Kasemo, B. *J. Phys. Chem.* **1993**, *97*, 12828.
(13) Försth, M.; Gudmundson, F.; Persson, J.; Rosén, A. *Combust. Flame* **1999**, *119*, 144.
(14) Gudmundson, F.; Persson, J.; Försth, M.; Behrendt, F.; Kasemo, B.; Rosén, A. *J. Catal.* **1998**, *179*, 420.
(15) Eisert, F.; Elg, A.-P.; Rosén, A. *Appl. Phys. A* **1995**, *60*, 209.
(16) Elg, A.-P.; Andersson, M.; Rosén, A. *Appl. Phys. B* **1997**, *64*, 573.
(17) Ljungström, S.; Hall, J.; Kasemo, B.; Rosén, A.; Wahnström, T. *J. Catal.* **1987**, *107*, 548.
(18) Johansson, Å.; Försth, M.; Rosén, A. *Surf. Sci.* **2003**, *529*, 247.
(19) Williams, W. R.; Marks, C. M.; Schmidt, L. D. *J. Phys. Chem.* **1992**, *96*, 5922.
(20) Hsu, D. S.; Hoffbauer, M. A.; Lin, M. C. *Langmuir* **1986**, *2*, 302.
(21) Zum Mallen, M. P.; Williams, W. R.; Schmidt, L. D. *J. Phys. Chem.* **1993**, *97*, 625.
(22) Anderson, L. C.; Mooney, C. E.; Lunsford, J. H. *Chem. Phys. Lett.* **1992**, *196*, 445.

(23) Wahnström, T.; Ljungström, S.; Rosén, A.; Kasemo, B. *Surf. Sci.* **1990**, *234*, 439.
(24) Hellsing, B.; Kasemo, B.; Ljungström, S.; Rosén, A.; Wahnström, T. *Surf. Sci.* **1987**, *189/190*, 851.
(25) Hellsing, B.; Kasemo, B.; Zhdanov, V. P. *J. Catal.* **1991**, *132*, 210.
(26) Försth, M. *Combust. Flame* **2002**, *130*, 241.
(27) Fridell, E.; Hellsing, B.; Ljungström, S.; Rosén, A.; Wahnström, T. *J. Vac. Sci. Technol., A* **1991**, *9*, 2322.
(28) Hu, R.; Huang, S.; Liu, Z.; Wang, W. *Appl. Surf. Sci.* **2005**, *242*, 353.
(29) Völkening, S.; Bedürftig, K.; Jacobi, K.; Wintterlin, J.; Ertl, G. *Phys. Rev. Lett.* **1999**, *83*, 2672.
(30) Försth, M.; Eisert, F.; Gudmundson, F.; Persson, J.; Rosén, A. *Catal. Lett.* **2000**, *66*, 63.
(31) Anton, B. A.; Cadogan, D. C. *Surf. Sci. Lett.* **1990**, *239*, L548.
(32) C*avity Ringdown Spectroscopy*; Busch, K. W., Busch, M. A., Eds.; ACS Symposium Series 720; American Chemical Society: Washington, DC, 1999.
(33) Marcus, G. A.; Schwettman, H. A. *Appl. Opt.* **2002**, *41*, 5167.
(34) Spaanjaars, J. J. L.; ter Meulen, J. J.; Meijer, G. *J. Chem. Phys.* **1997**, *7* 107.
(35) Mercier, X.; Therssen, E.; Pauwels, J. F.; Desgroux, P. *Chem. Phys. Lett.* **1999**, *299*, 75.
(36) Mercier, X.; Pillier, L.; Bakali, A.; Carlier, M.; Pauwels, J. F.; Desgroux, P. *Faraday Discuss.* **2001**, *119*, 305.
(37) Dreyer, C. B.; Spuler, S. M.; Linne, M. *Combust. Sci. Technol.* **2001**, *171*, 163.
(38) Evertsen, R.; Stolk, R. L.; Ter Meulen, J. J. *Combust. Sci. Technol.* **1999**, *149*, 19.
(39) Luque, J.; Jeffries, J. B.; Smith, G. P.; Crosley, D. R.; Scherer, J. J. *Combust. Flame* **2001**, *126*, 1725.
(40) Luque, J.; Berg, P. A.; Jeffries, J. B.; Smith, G. P.; Crosley, D. R.; Scherer, J. J. *Appl. Phys. B* **2004**, *78*, 93.
(41) Naik, S. V.; Laurendeau, N. M. *Appl. Opt.* **2004**, *43*, 5116.
(42) Bahrini, C.; Douin, S.; Rostas, J.; Taieb, G. *Chem. Phys. Lett.* **2006**, *432*, 1.
(43) Hagemeister, F. C.; Arrington, C. A.; Giles, B. J.; Quimpo, B.; Zhang, L.; Zweier, T. S. *Cavity Ringdown Spectroscopy*; Busch, K. W., Busch, M. A., Eds.; ACS Symposium Series 720; American Chemical Society: Washington, DC, 1999; pp 210−232.
(44) Hemdal, S.; Johansson, Å.; Försth, M.; Andersson, M.; Rosén, A. *J. Vac. Sci. Technol., A* **2004**, *22*, 1620.
(45) O'Keefe, A.; Deacon, D. A. G. *Rev. Sci. Instrum.* **1988**, *59*, 2544.
(46) Meijer, G.; Boogaarts, G. H.; Jongma, R. T.; Parker, D. H.; Wodtke, A. M. *Chem. Phys. Lett.* **1994**, *217*, 112.
(47) Yu, T.; Lin, M. C. *J. Am. Chem. Soc.* **1993**, *115*, 4371.
(48) Yu, T.; Lin, M. C. *J. Phys. Chem.* **1994**, *98*, 2105.
(49) Berden, G.; Peeters, R.; Meijer, G. *Int. Rev. Phys. Chem.* **2000**, *19*, 565.
(50) Fallows, E. A.; McAndrew, B.; Miller, J. H. *Chem. Phys. Processes Combust.* **2005**, 231.
(51) Scherer, J. J.; Paul, J. B.; O'Keefe, A.; Saykally, R. J. *Chem. Rev.* **1997**, *97*, 25.
(52) Cheskis, S.; Derzy, I.; Lozovsky, V. A.; Kachanov, A.; Romanini, D. *Appl. Phys. B* **1998**, *66*, 377.
(53) Wheeler, M. D.; Newman, S. M.; Orr-Ewing, A. J.; Ashfold, M. N. R. *J. Chem. Soc., Faraday Trans.* **1998**, *94*, 337.
(54) Zalicki, P.; Zare, R. N. *J. Chem. Phys.* **1995**, *102*, 2708.
(55) Luque, J.; Crosley, D. R. *LIFBASE*, version 1.45; SRI International: Menlo Park, CA, 1998.
(56) Eckbreth, A. C. *Laser Diagnostics for Combustion Temperature and Species*; Gordon and Breach Science Publishers: Amsterdam, The Netherlands, 1996.
(57) Dimpfl, W. L.; Kinsey, J. L. *J. Quant. Spectrosc. Radiat. Transfer* **1979**, *21*, 233.
(58) Fridell, E.; Rosén, A.; Kasemo, B. *Langmuir* **1994**, *10*, 699.
(59) Crosley, D. R. *Opt. Eng.* **1981**, *20*, 511.
(60) Kohse-Höinghaus, K. *Prog. Engery Combust. Sci.* **1994**, *20*, 203.
(61) Jeffries, J. B.; Kohse-Höinghaus, K.; Smith, G. P.; Copeland, R. A.; Crosley, D. R. *Chem. Phys. Lett.* **1988**, *152*, 160.